JOURNAL OF OPTOELECTRONICS AND ADVANCED MATERIALS, Vol. 11, No. 7, July 2009, p. 964 - 969

Effect of Fe doping concentration on electrical and magnetic properties of ZnO nanoparticles prepared by solution combustion method

M. L. DINESHA*, H. S. JAYANNA, S. ASHOKA[a], G. T. CHANDRAPPA[a]
Departrment of PG Studies and Research in Physics, Kuvempu University, Shankaraghatta-577451, Karnataka, India
[a]Department of Chemistry, Central College Campus, Bangalore University,Bangalore-560001, Karnataka, India

Nano-sized Fe doped ZnO ($Zn_{1-x}Fe_xO$ where x=0.00, 0.005, 0.01, 0.02, 0.03, 0.04) powders were prepared by simple solution combustion method. The powder X-ray diffraction patterns of these samples showed that they are single phase without any secondary phases. The DC electrical conductivity measurements were carried out in the temperature range 300 K-650 K and it was found to increase with increase of temperature. At room temperature, DC electrical conductivity was evidenced to decrease with increase in Fe content. The hysteresis in the M-H behavior shows the presence of room temperature ferromagnetism in Fe doped ZnO.

(Received February 2, 2009; accepted July 20, 2009)

Keywords: Spintronics, Solution combustion, Electrical conductivity, Magnetic properties

1. Introduction

In the last few years, there has been growing research on the investigations of nanostructures. Progress has been achieved in the synthesis, structural characterization and physical properties of nanostructures. These nanomaterials, due to their peculiar characteristics and size effects often show novel physical properties compared to those of bulk. These potentialities can be exploited both for fundamental study and for potential nanodevice applications. The potentialities of these innovative structures are being exploited also for electrical and magnetic applications. Today, nanoparticles of metal oxides have been the focuses of a number of research efforts due to the unusual properties that are expected upon entering this size regime. In the field of spintronics, it is believed that the usefulness of ferromagnetic wide band gap semiconductors requires the existence of a coupling between ferromagnetic and semiconducting properties. As a result, dilute magnetic semiconductors produced by doping transition metal ion into nonmagnetic semiconductor had drawn much attention.

Zinc oxide (ZnO) is an n-type metal oxide semiconductor with a wide band gap (3.37 eV) having properties suitable for various applications such as ultraviolet opto-electronic devices, transparent high power and high frequency electronic devices, piezoelectronic transducers and chemical gas sensors [1-5]. The study about the effect of dopants on physical and electrical properties of electronic components such as piezoelectronic transducers and varister is very important. The electrical properties of ZnO are very much dependent on the composition and its structure. There are some reports on the effect of various transition metals on the conductivity of bulk ZnO prepared by several methods [6-7].

Recently, a significant interest has been exhibited in achieving magnetic functionality in ZnO. Transition metal-doped ZnO has been investigated as a promising dilute magnetic semiconductor for implementing spintronic device concepts. The Room temperature (RT) ferromagnetism in Fe doped ZnO is still in debate. Han et al. failed to obtain RT ferromagnetism in Fe doped ZnO bulk samples and suggested that additional Cu doping is essential to achieve RT ferromagnetism in these samples [8]. However Y Q Wang et al. observed RT ferromagnetism in Fe doped ZnO bulk samples prepared by co-precipitation method [9]. Hence, in the present work, we have reported the DC electrical conductivity and magnetic properties of $Zn_{1-x}Fe_xO$ powder samples prepared by a simple solution combustion method.

2. Experimental

The Combustion method has been considered to be fast, simple and inexpensive, allowing for the production of fine, homogeneous crystalline powders without the risk of contamination. The $Zn_{1-x}Fe_xO$ (where x=0.00, 0.005, 0.01, 0.02, 0.03, 0.04) powders were prepared by solution combustion method using stoichiometric composition of metal nitrates (AR grade) as oxidizers and glycine as a fuel. The aqueous solution containing redox mixture was

taken in a Pyrex dish and heated in a muffle furnace maintained at 400 ± 10 °C. The mixture finally yields porous and voluminous powder. The following chemical reaction taken place during the synthesis,

$$Zn(NO_3)_2 + Fe(NO_3)_2 \xrightarrow[\text{water}]{\text{glycine}} Zn_{1-x}Fe_xO + \text{gaseous products}$$

These powder samples were characterized by Powder X-Ray Diffraction (PXRD) patterns using Cu-Kα radiation (λ=1.5418 Å). The scanning rate was 0.05° per step and the measuring times 15 s./step. The average particle size can be determined by using Scherrer's equation,

$$d = 0.9\lambda / \beta \cos\theta \quad (1)$$

where d =Size of the particle, θ = Glancing angle (2θ/2) and β = Full width half maxima.

Surface morphology was studied by scanning electron microscope (SEM).

For electrical conductivity study, the powder samples were mixed with PVA binder and then pressed uniaxially into a pellet of thickness 1-2 mm and of diameter 10 mm by applying pressure of 120 MPa for 3 min. The pellets were sintered at 300 ^{0}C for 3 hrs to remove the added binder. Fine quality silver paint was applied on both sides of the pellets for good electrical contacts. The DC electrical conductivity study is carried by two probe method using KEITHLEY source meter (model 2400) in the temperature range 300 K-650 K. The measurements were recorded during heating cycle. The electrical conductivity σ is calculated by the formula

$$\sigma = I t / V A \quad (2)$$

where V is the applied voltage, I is the measured current, A is the area of the pellet and t is thickness of the pellet.

The Arrhenius equation which relates the electrical conductivity and the temperature is given by

$$\sigma = \sigma_0 \exp\{-E_a/K_B T\} \quad (3)$$

where E_a is the activation energy, K_B is Boltzmann constant, and T is the temperature. The activation energy is calculated from Arrhenius plot.

The room temperature magnetic property was studied from vibrating scanning magnetometer by applying the magnetic field up to 2.5KOe.

3. Result and discussion

3.1. Structural characterization

The polycrystalline powder samples were characterized by PXRD and the diffraction patterns are shown in Fig. 1. All the PXRD peaks can be indexed to a wurtzite structure of ZnO. From Fig. 1 it is evident that the doping of Fe on ZnO cannot change the wurtzite structure of ZnO. No extra peaks are found in the pattern indicating the formation of single phase $Zn_{1-x}Fe_xO$. A small shift in the position of main peak (101) to the lower side of 2θ value is observed for doped samples. This observation is similar to the case in transition metal (Mn, Cu, and Ni) doped ZnO studied by S Ekambaram et al. [10]. This shift is mainly due to the larger radius of Fe^{3+} than Zn^{2+}. This indicates that the doped Fe atoms substitute Zn atoms. The particle size of the samples calculated using Scherrer's formula and is found to be in the range of 19-34 nm.

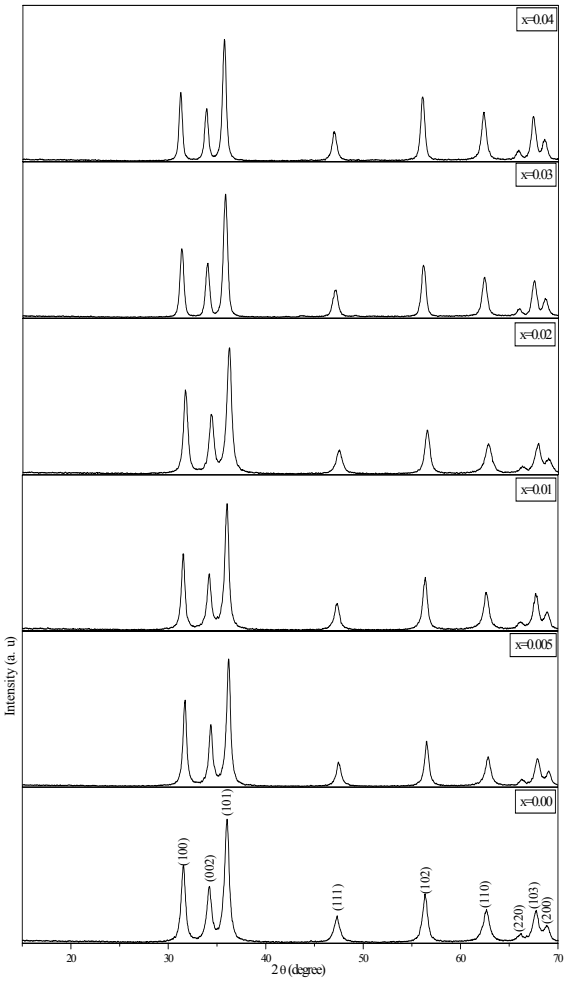

Fig. 1. PXRD patterns of $Zn_{1-x}Fe_xO$

Fig. 2(a) and (b) shows the SEM images of nanocrystalline ZnO and doped Fe ZnO respectively. The SEM image of pure ZnO powder exhibits cluster of tiny particles having diameters in the range 10-30 nm. From the Fig. 2(b), it is observed that the Fe doped ZnO powder is highly porous. The high porosity is attributed due to the

liberation of gaseous products like H_2O, CO_2 and N_2 during combustion process.

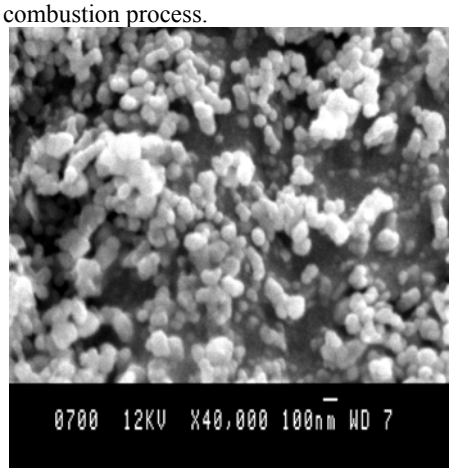

(a)

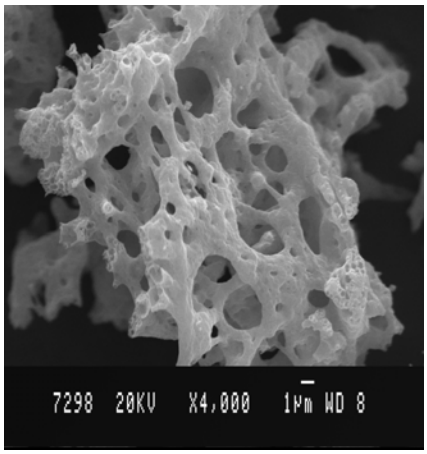

(b)

Fig. 2. (a) ZnO and (b) Fe doped ZnO SEM images of combustion derived nanoparticles

3.2. DC Electrical characterization

The DC electrical conductivity of $Zn_{1-x}Fe_xO$ samples at room temperature is shown in Fig. 3. It is observed that the conductivity decreases with increase of Fe concentration and it is high for undoped ZnO. It is well known that the electrical conductivity of ZnO samples at room temperature is due to intrinsic defects created by oxygen vacancies. These defects introduce donor states in the forbidden band slightly below the conduction band and hence resulting in the conducting behavior of ZnO. This electrical conductivity is controlled by the intrinsic defects generated during synthesis and by the presence of dopants. It is known that during combusting process usually a high temperature (more than 1000^0C) will be produced resulting in the generation of oxygen vacancies which are responsible for electrical conductivity. From the observed result of decrease in conductivity of ZnO on Fe doping, it seems that the Fe doping affects the defect chemistry of the ZnO [11]. Therefore, we may believe that Fe in ZnO acts as a deep donor and decreases the concentration of intrinsic donors at combustion temperature resulting in the decrease of electrical conductivity. This reduction in the intrinsic donor concentration increases with increase of Fe content and hence results in the decrease of conductivity with an increases of Fe concentration.

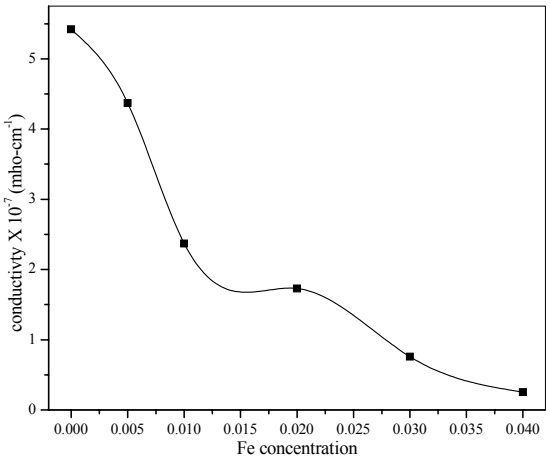

Fig. 3. Variation of room temperature electrical conductivity with Fe concentration

The temperature dependence of electrical conductance of $Zn_{1-x}Fe_xO$ is shown in Fig. 4. It is found that conductivity increases with increase of temperature and hence showing the semiconducting behavior of pure and Fe doped ZnO samples. Anyhow, conductivity curve can be divided in to two regions based on conductivity variation. In case of pure ZnO, conductivity raises slowly with increase of temperature up to 400 K, later drastic increase in conductivity has been observed. But in case of Fe doped ZnO the conductivity variation is slow up to 550 K later it increases drastically.

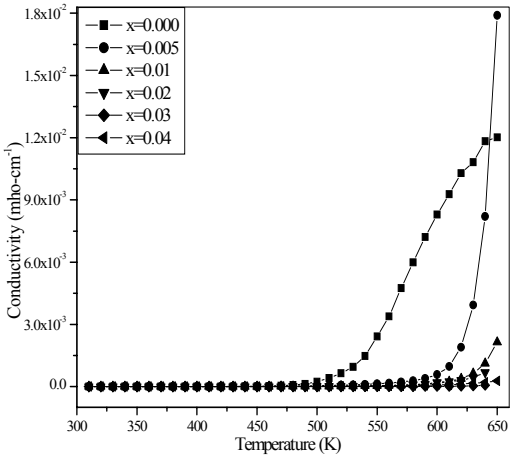

Fig. 4. Variation of electrical conductivity with temperature

The observed two-stage temperature dependence of conductance σ may be represented as:

$$\sigma = \sigma_L \exp\left\{-\frac{E_{aL}}{K_B T}\right\} + \sigma_H \exp\left\{-\frac{E_{aH}}{K_B T}\right\} \quad (4)$$

In Equation (4), σ_L and σ_H are pre-exponential factors, E_{aL} and E_{aH} are the activation energy for low and high temperature conductance stages respectively. Fig. 5(a) and Fig. 5(b) shows the Arrhenius plot of pure ZnO and Fe doped ZnO respectively and calculated activation energies are given in Table 1. For pure ZnO the calculated values of E_{aL} and E_{aH} are 0.47eV and 0.97eV respectively. In case of Fe doped ZnO these values are 0.52-0.61 eV and 1.17-1.29 eV respectively and these values are increases with increase of Fe concentration.

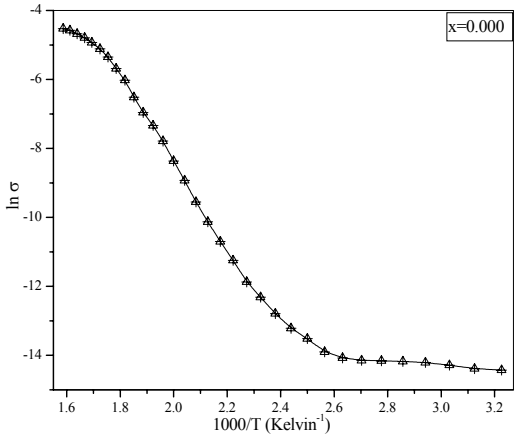

(a)

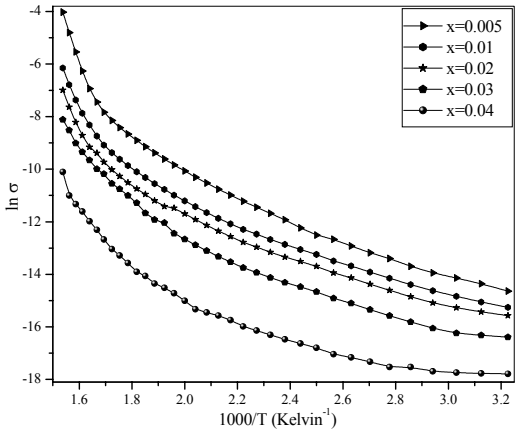

(b)

Fig. 5. (a) ZnO and (b) Fe doped ZnO Arrhenius plots

Table 1. Experimental values of electrical conductivity, activation enrgy, magnetic moment for different concentration of Fe.

x(%)	Room temperature electrical conductivity (X 10^{-7} mho-cm^{-1})	Activation Energy (eV)		Magnetic moment (emu/gm)	Average particle size (nm)
		E_{aL}	E_{aH}		
0.00	5.42	0.47	0.97	---	19
0.5	4.37	0.52	1.17	20.67	21
1	2.37	0.53	1.20	7.55	24
2	1.73	0.56	1.23	7.43	28
3	0.759	0.59	1.25	5.13	31
4	0.254	0.61	1.29	4.85	34

The low temperature activation energy of ZnO samples is possibly associated with one of the following two donor ionization processes:

$$V_O \rightarrow V_O^+ + e^- \quad (5)$$

proposed by Simpson and Cordaro [12] for oxygen vacancy (Vo) or,

$$Zn_i^+ \rightarrow Zn_i^{++} + e^- \quad (6)$$

proposed by Sukker and Tuller [13] for zinc interstitial (Zn_i) which forms a donor level 0.47 eV below the conduction band. In case of doped ZnO, one of these two forms a donor level 0.52-0.61 eV below the conduction band.

The high temperature activation energy can be associated with desorption of O_2^- species [14] according to the equation,

$$O_2^- \rightarrow O_2 + e^- \quad (7)$$

Later, the increase in the activation energy of Fe doped ZnO can be explained as follows: When ZnO is substituted with Fe ions which are in 3+ ion state replaces the Zn^{2+} ions and occupies zinc interstitial sites. The substituted Fe ions cannot be easily ionized as like Zinc ions because of their higher ionization potential (2eV). Hence, the donor concentration is lowered by addition of Fe which results in the decrease of electrical conductivity. Thus, higher value of activation energy (E_a) is found for Fe doped ZnO samples and it increases with increase of iron concentration (x).

3.3. Magnetic hysteresis study

Fig. 6 (a)-(e) shows the magnetic hysteresis (M-H) curves of Fe doped ZnO at 300K. From the figures, hysteresis behavior is clearly observed and consistent with ferromagnetism which is contrary to earlier report [8]. Area of the loop decreases with increase of Fe concentration. The saturated magnetic moment values of

all these samples are given in the Table1. Increasing the Fe content from 0.5% to 4% resulted in a decrease in the relative magnetization response. Also PXRD study reveals the formation of no secondary phase in these samples. This provides the strong evidence that the magnetization in Fe doped ZnO is not due to any secondary phase like formation of Fe cluster or Fe_2O_4. If the metallic iron or iron oxides were responsible for the observed ferromagnetic behavior, an increase in Fe concentration would presumably increase the corresponding magnetic moment values. Instead, the opposite behavior is observed suggest that the observed room temperature ferromagnetism in $Zn_{1-x}Fe_xO$ is an intrinsic behavior, independent of secondary phase formation.

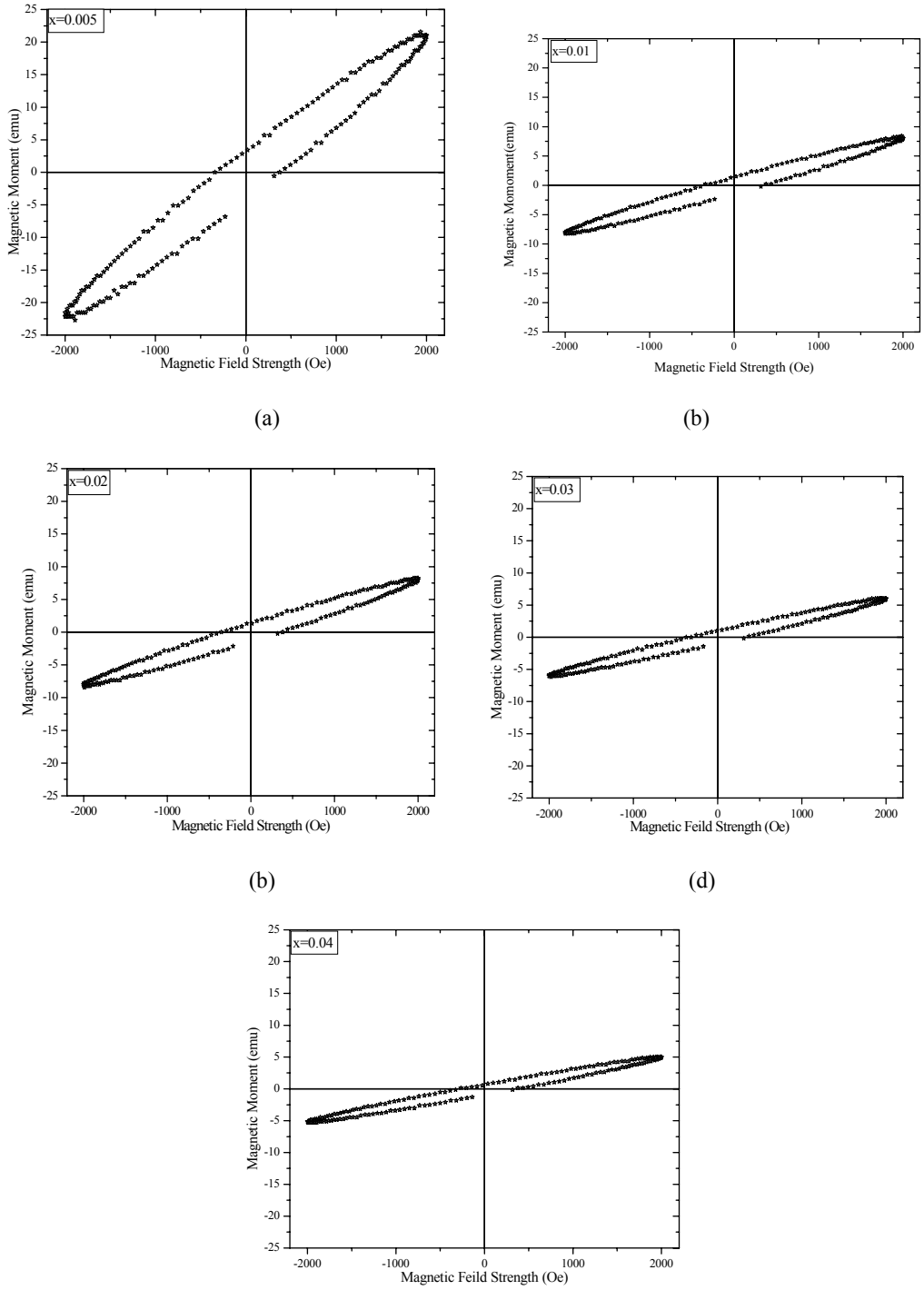

Fig. 6. (a)-(e) Magnetic hysteresis (M-H) loops of $Zn_{1-x}Fe_xO$ at room temperature under 2.5 kOe.

In view of this, the substitution of Fe^{3+} for Zn^{2+} Carrier-mediated ferromagnetism has a possibility to explain the observed magnetic behavior in Fe doped ZnO [15]. The theory [16, 17] based on interaction between magnetic polarons is another candidate. Disorder [18-19] defects may also be an important factor for the observed ferromagnetism in $Zn_{1-x}Fe_xO$. A detailed research is required on this problem to clarify the doubt.

4. Conclusion

Single phase Fe doped ZnO in nanoscale were prepared by solution combustion method and confirmed by PXRD analysis and surface morphology was studied by SEM. The Fe doping reduces the electrical conductivity of pure ZnO nanomaterials. The electrical conductivity decreases with increase of Fe concentration. The magnetic hysteresis loops at room temperature confirms the presence of ferromagnetism in Fe doped ZnO. The introduction of Fe transition metal into these materials under the right condition is found to produce ferromagnetism at the room temperature. The present behavior is an intrinsic property of Fe doped ZnO. The presence of ferromagnetism in Fe doped ZnO nanomaterials prepared via simple solution combustion method offers a new potentiality in spintronics applications.

Acknowledgements

Authors are thankful to Prof. B K Chougule, Department of Physics, Shivaji University, Kolhapur, India for providing the facility of magnetic hysteresis measurements.

References

[1] J. Joo, S.G. Kwon, J.H. Yu, and T. Hycon, Adv. Mater. **15**, 1873 (2005).
[2] U. Pal, and P. Santiago, Phys. Chem. B **109**, 15317 (2005).
[3] L. Vayssieres, Adv. Mater. **15**, 464 (2003).
[4] L. Vayssieres, A. Hagfeldt, and S.E. Lindquist, Chem. Mater. **13**, 4395 (2001).
[5] G. Marcì, V. Augugliaro, M.J. Lopez-Munoz, C. Martin, L. Palmisano, V. Rives, M. Schiavello, R.J.D. Tilley, and A.M. Venezia, J. Phys. Chem. **105**, 1026 (2001).
[6] A.M.R. Jiang Han, P.Q. Senos, Mantas, J. of the European Ceramic Society **22**, 1653 (2002).
[7] M. Sedky, Abu-Abdeen, A. Abdalaziz, Almulhem, Physica B **388**, 266 (2007).
[8] S.J. Han, J.W. Song, C.H. Yang, S.H. Park, J.H. Jeong, Appl. Phys. Lett. **81**, 4212 (2002).
[9] Y.Q. Wang, Z.L. Yuan, L. Liu, X.X. Lan, Z.M. Tian, JH He, S.Y. Yin, J. Magnetism and Magnetic Materials, **320**, 1423 (2007).
[10] S. Ekambaram, Yoichi Iikubo, Akihiko Kudo, J. Alloys & compounds, **433**, 237 (2006).
[11] T.K. Gupta, J. Mater. Res. **7**, 3280 (1992).
[12] J.C. Simpson, and J.F. Cordero, Appl. Phys. **63**, 1781 (1988).
[13] M.H. Sukker, and H.L. Tuller, Defect equilibria in ZnO varistor materials, Advances in Ceramics, Advances in Ceramics, **7**, 49 (1984).
[14] Satoru Fujitsu, Kunihito Koumoto, Hiroaki Yanagida, Yuichi Watanabe and Hiroshi Kawazoe, J. Appl. Phys. **38**, 1534 (1999).
[15] X.X. Liu, F.T. Lin, L.L. Sun, W.J. Chen, X.M. Ma, W.Z. Shi, Appl. Phys. Lett. **88**, 062508 (2006).
[16] A.C. Durst, R.N. Bhatt, P.A. Wolff, J. Appl. Phys. **79**, 5196 (1996).
[17] A. Kaminski, S. Das Sarma, Phys. Rev. Lett. **88**, 247202 (2002).
[18] M. Berciu, R.N. Bhatt, Phys. Rev. Lett. **87**, 107203 (2001).
[19] A.L. Chudnovskiy, D. Pfannkuche, Phys. Rev. B **65**, 165216 (2002).

*Corresponding author: dmlsagar@gmail.com